

Photoemission study of iron deposited on fullerenes

M. W. Ruckman, Bo Xia, and D. Shih

Physics Department, Brookhaven National Laboratory, Upton, New York 11973

(Received 7 June 1994; revised manuscript received 19 September 1994)

Photoelectron spectroscopy is used to study iron particles grown by depositing Fe on a fullerene film. For small amounts of iron deposited on the fullerenes, the Fe 3*p* core level is shifted ~ 0.4 eV to greater binding energy and a clear Fermi edge is missing. Theoretical studies by other workers, principally calculations of the electronic structure for small clusters, suggest that the iron is dispersed in the fullerene matrix in the form of small clusters. When the amount of Fe increases and the clusters become larger, some of the Fe valence states move towards E_f and the valence band develops a Fermi edge indicative of metallization.

Iron-containing clusters and particles have unique physical and chemical properties of interest to those making magnetic recording media¹ and catalysts.² There have been many experimental and theoretical studies of iron particles. For example, various theoretical methods have been applied to compute the electronic structure of iron particles and deduce properties like the magnetization.³ Cluster beam experiments have provided detailed information about cluster structure and the magnetic moment as a function of cluster size.⁴ Spectroscopic studies of small iron particles on a variety of surfaces have been done to determine their electronic and magnetic properties.⁵⁻⁸

This paper describes a photoelectron study of iron clusters grown on a thick fullerene film. To the best of our knowledge, such studies of Fe in fullerenes have not been published and there have been few, if any, photoelectron studies of iron isolated as clusters in any "inert" matrix. Photoelectron spectroscopy was used to study the evolution of the Fe valence electronic states. Fullerenes were used to isolate the Fe atoms for cluster growth, in part, because it has also been shown that many transition metals do not react with fullerenes and form clusters.⁹ In similar experiments with palladium deposited on fullerenes, we have found that a larger number of palladium atoms can be assembled into small clusters because the fullerene matrix seems to prevent the rapid agglomeration which occurs when the same atoms are deposited in xenon.¹⁰ An advantage of using fullerenes instead of noble gases to isolate clusters is that the fullerene solid exists at room temperature and could be heated to several hundred °C for temperature-programmed desorption (TPD) experiments of gases adsorbed on the small iron particles. This cannot be done using condensed rare gases like Xe or Kr which would evaporate, and also cannot be done with iron particles or islands supported on graphite or mica because the clusters are mobile and agglomerate.

The experimental work was done in ultrahigh vacuum (1×10^{-10} -Torr base pressure) chamber of standard design at the National Synchrotron Light Source (NSLS) (U7b beam line). A hemispherical electron energy

analyzer was used to detect and analyze the photoelectrons produced by a photon beam which was incident on the surface at an angle of 45°. Photoelectrons emitted within 2° of the surface normal were detected by the analyzer, which was operated at 25-eV pass energy. The spectral resolution was limited by the monochromator and was estimated to be ~ 0.5 eV [as deduced from the full width at half maximum (FWHM) of the Ta Fermi edge]. All spectra are referenced to the Fermi level (E_f) of the tantalum support.

The fullerene films were grown on a tantalum strip that was cleaned by heating to incandescence. The cleanliness of the tantalum substrate was checked by photoemission examination of the Ta 4*f* core levels and the Ta valence band which are very sensitive to small amounts of contamination.¹¹ The fullerene films were made by the sublimation of a commercial fullerene powder. The starting fullerene material was 80% by weight C₆₀ and 20% by weight other fullerenes and soot. The fullerene powder was placed inside a tantalum foil tube with perforations to allow the fullerenes to escape. A K-type thermocouple was spot welded to the tube and used to monitor and control the temperature. It is known that pure C₆₀ can be distilled from the mixture of fullerenes and soot. Photoelectron spectroscopy showed that a relatively pure C₆₀ fullerene film was deposited when the source temperature ranged from 480 to 490 °C.

The iron films were deposited on thick fullerene films (i.e., thick enough to block photoelectrons from the Ta support) using a filament source made by winding a Fe strand around a tungsten filament. The resistively heated Fe filament was always operated at constant power (~ 15 W), and after sufficient outgassing produced a clean iron film. The amount of iron was estimated from timing the duration of each deposition done under conditions of constant filament power and multiplying that time by a scale factor to convert from time to thickness in monolayers. The scaling factor was deduced from the attenuation of the Ta 4*f* core-level photoemission when iron films were deposited on Ta(110) under the same conditions. For an attenuation factor of $1/e$, we assumed that the photoelectron mean free path was ~ 5 Å or ~ 2 mono-

layers. The scaling factor was deduced from the attenuation of the Ta 4f core-level photoemission when iron films were deposited on Ta(110) under the same conditions. For an attenuation factor of $1/e$, we assumed that the photoelectron mean free path was $\sim 5 \text{ \AA}$ or ~ 2 monolayers (ML) ($1 \text{ ML} = \sim 1.3 \times 10^{15} \text{ Fe atoms/cm}^2$).

Figure 1 shows typical Fe 3p core-level results for iron vapor deposited on a fullerene. The Fe 3p core-level data was taken at a photon energy of 120 eV. For Fe deposited on C_{60} , the Fe 3p core levels are shifted ~ 0.4 eV to greater binding energy when compared to metallic iron which has a binding energy of -52.7 eV.¹² The shift of the Fe 3p peak to higher binding energy could be due to the finite size of the clusters or particles. It is well known that the potential for a surface atom differs from the bulk due to the lower coordination number.¹³ For early (less

than half-filled *d* band) transition metals, the core levels shift to higher binding energy, whereas for late (more than half-filled *d*-band) transition metals the shift is to lower binding energy. In this experiment the shift of the Fe 3p is to higher binding energy—not to lower binding energy as would be expected from its position in the Periodic Table. The shift of the Fe 3p core level to higher binding energy could be due to a small amount of charge transfer from the iron to the fullerene. When iron interacts with other elements and forms divalent or trivalent compounds, the core level shifts to higher binding energy. For example, the divalent and trivalent oxides (FeO and Fe_2O_3) have Fe 3p core levels at -55.6 and -57.6 eV binding energy, respectively.^{14,15} The magnitude of the core-level shift is a fraction of that observed for the two iron oxides (0.43 compared to 2.9 or 4.9 eV, respectively).

The core-level binding energies of materials isolated in nonmetallic matrices can change because charging of the material (i.e., the metal particle or cluster) can take place. In a study of Pt isolated in silica by Murgai *et al.*,¹⁶ the authors argued that most of the Pt 4f_{7/2} core-level shift was due to a Coulomb effect related to the finite size of the cluster. When clusters are isolated and neutralization of the core hole is slow on the time scale of the photoemission event, the outgoing photoelectron will see the positive charge and be slowed by the factor $e^2/2\epsilon r$ (Coulomb energy), where e is the electron charge, r is the radius of the cluster, and ϵ is the dielectric constant. The reduction in the kinetic energy of the outgoing photoelectron will manifest itself as a shift of the core level to greater binding energy. In the case of Fe in C_{60} , the dielectric constant is 4.4,¹⁷ and the core-level shift is ~ 0.4 eV to greater binding energy. If it is assumed that all of the core-level shift is due to the Coulomb energy term, it can be shown that the iron clusters would have to be $\sim 10 \text{ \AA}$ in diameter.

Valence-band spectra for increasing amounts of Fe on the fullerenes are shown in Fig. 2. The bottom curve shows a spectrum for a pure fullerene film that contains mostly C_{60} . The electronic structure and photoemission from such films have been thoroughly studied and described in detail by others.^{18,19} Assuming the film is predominantly C_{60} , the two peaks nearest the Fermi level (marked by solid vertical lines) have π -like character, while the peaks (marked with dashed lines) extending from -5 - to -15 -eV binding energy have more σ -like character. The deposition of iron into the fullerene material causes the fullerene peaks to broaden. The greatest changes in the spectra are seen in the region where the Fe 3d and fullerene peaks overlap. A broad feature attributed to the Fe 3d states grows and obscures the two lowest binding-energy fullerene peaks. Unlike the valence states of pure iron²⁰ (Fig. 2, top curve), the density of Fe 3d states near the Fermi level for monolayer coverage seem much smaller, and, at the lowest coverage studied (0.2 ML), no Fermi edge is seen.

The changes in the Fe 3d states near E_f are more clearly seen in difference curves (inset in Fig. 2) plotted on an expanded energy scale to highlight the region of interest near E_f . The first Fe deposition ($\theta=0.2$ ML), pro-

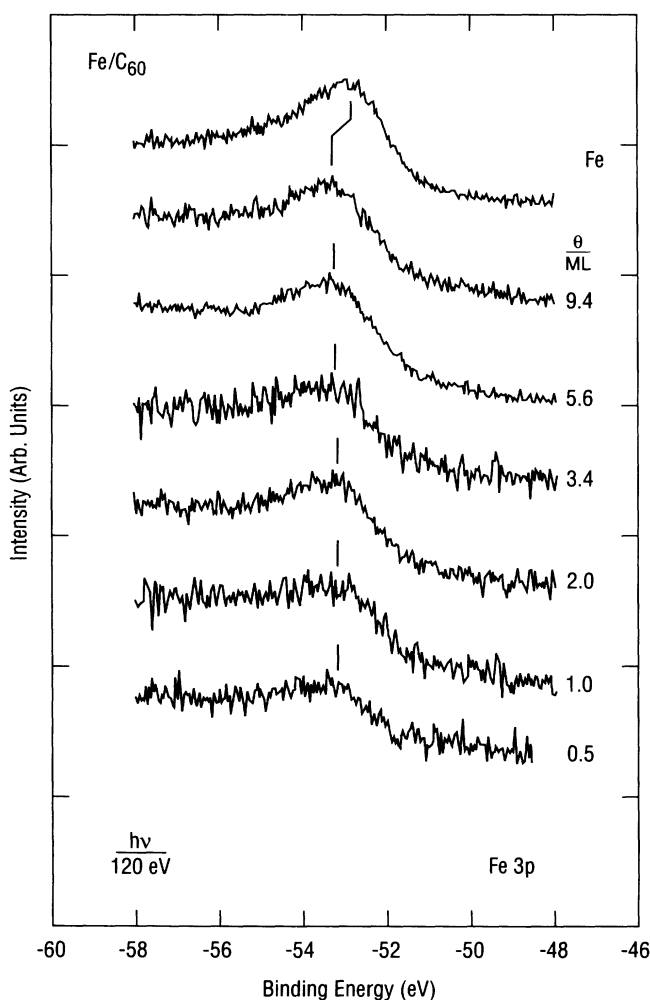


FIG. 1. The figure shows Fe 3p core-level spectra taken at $h\nu = 120$ eV for a pure iron film (top curve) and for iron coverages ($0.5 < \theta < 9.4$ ML) on a thick fullerene film. Iron film thicknesses were deduced from the evaporation time and a scale factor based on the prior study of an iron epilayer grown on Ta(110). The Fe 3p binding energy is referenced to the Fermi edge of the Ta support. When the iron is dispersed on the fullerene layer the core-level shifts -0.43 eV to higher binding energy.

duces a distribution of states (marked by circles) which extends into the gap between the topmost fullerene peak and the Fermi level. There is no indication of a step in the Fe 3d states at the Fermi energy. The appearance of the Fe 3d states resembles that of a nonmetallic material. Adding more iron to the fullerenes (0.5 ML), increases the intensity of the Fe 3d component (marked by squares) and produces the first hint of a Fermi edge. A clear Fermi edge is seen when the amount of iron (triangles) is increased to that needed to form a monolayer. The top-most curve (inset in Fig. 2) reproduces the photoelectron spectrum of pure iron (black diamonds). When the pure iron spectrum is compared to the spectra for the iron particles in the fullerene matrix, it can be seen that the Fe 3d states are shifted ~ 0.5 eV farther below the Fermi edge. The evolution of the Fe 3d valence states with increasing iron coverage can be attributed to two physical processes. The first is the growth of the iron clusters and the increased Fe 3d-4s hybridization as the electronic structure approaches that of metallic iron. The second is the decreased interaction between the iron and the fullerenes as the iron atoms acquire more Fe nearest neighbors. It is likely that a range of cluster sizes is produced and that

some of the clusters have reached the metallic state before others.

The electronic and magnetic electronic structures of small iron clusters have been studied theoretically.^{21,22} Such work for iron clusters (Fe_n) in a variety of fcc and bcc structures suggests that the electronic structure is very dependent on cluster size. Pastor, Dorantes-Davila, and Bennemann²¹ found that the local density of states at the Fermi level decreased in going from Fe_{27} to Fe_{15} clusters in the bcc structure. Pastor, Dorantes-Davila, and Bennemann²² also found that the cohesive energy decreased from 2.0 eV for bulk iron to 1.62 eV for the Fe_{15} cluster, and that the magnetic moment increased from $2.21 \mu_B$ to $2.58 \mu_B$. The magnetic moment undergoes rapid variations in strength depending on whether the atomic shells are complete or not. Mössbauer and x-ray-absorption fine-structure (XAFS) spectroscopy have been used to study the connection between local the magnetic moment and atomic structure. Montano *et al.*²³ found that iron clusters down to nine atoms in size have the bcc structure but transform to a fcc or hcp structure for the smaller clusters. To the best of our knowledge, a photoelectron study of iron clusters in a rare-gas matrix or on

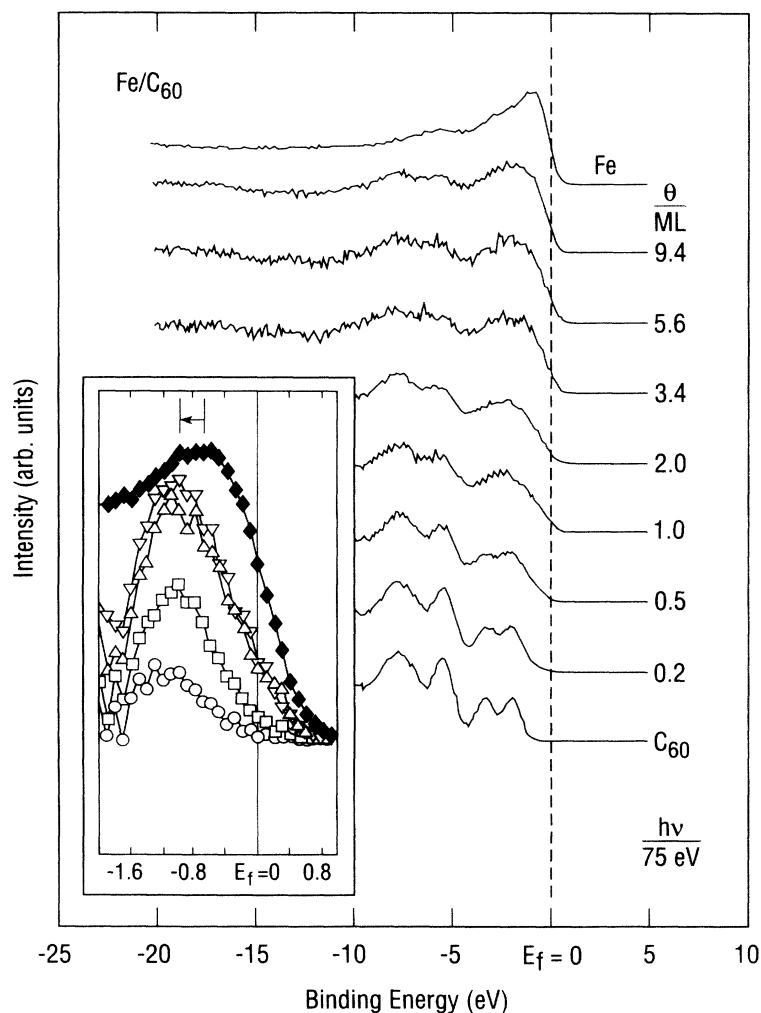


FIG. 2 Valence-band photoelectron energy distribution curves (EDC's) for a thick fullerene film (bottom curve), the pure iron film (top curve), and for iron coverages ($0.5 < \theta < 9.4$ ML) on the thick fullerene film. When iron is deposited on the fullerenes, the Fe 3d states overlap the two fullerene peaks closest to the Fermi edge reference. The inset reports data for the pure iron film rescaled for comparison (black diamonds) with difference curves designed to show the evolution of the Fe 3d-related states for Fe on the fullerenes. The difference curves are (1) 0.2–0 ML (white circles), (2) 0.5–0 ML (white squares), and (3) 1.0–0 ML (white triangles).

graphite has not been reported. However, Colbert²⁴ used photoelectron spectroscopy to study the evolution of the electronic structure of Ni when isolated in a xenon matrix. Nickel, like iron, has a partially filled *d* band. For Ni in xenon, Ni 3*d* emission appeared -1.4, -2.8, and -0.4 eV below the Fermi-level reference energy, and a Fermi edge was not observed. The result for Fe isolated in the fullerenes is similar to that observed for Ni in xenon, which like iron has a partially filled *d* band.

The findings presented in this paper show that iron clusters can be grown in fullerenes. Using work by others as a guide, we conclude the iron is well dispersed, and feel the clusters are small. The smaller clusters seen at the beginning of cluster growth show Fe 3*d* states shifted away from the Fermi level and lack a Fermi surface. The

Fermi edge appears as some of the clusters grow larger, which is in agreement with theory and experiments with other transition metals.

D.S. acknowledges support from the U.S. Department of Energy's Division of University and Industry Programs, Office of Energy Research, as a Science and Engineering Research Semester (SERS) Program participant. The experimental work was done at the National Synchrotron Light Source supported by the U.S. Department of Energy, Division of Materials Sciences. The work was funded by the U.S. Department of Energy, Division of Materials Sciences under Contract No. AC02-76CH00016.

¹For examples, see *Small Particles and Inorganic Clusters, Proceedings of the 4th International Meeting on Small Particles and Inorganic Clusters, Aix-en-Provence, France, 1988*, edited by C. Chaperon, M. F. Gilet, and C. R. Henry [*Z. Phys. D* **12**, 1 (1989)].

²M. Boudart, A. Delbonille, J. A. Dumesic, S. Khammouna, and H. Topsbe, *J. Catal.* **37**, 486 (1975).

³G. M. Pastor, J. Dorantes-Davila, and K.-H. Bennemann, *Phys. Rev. B* **40**, 7642 (1989); K. Lee, J. Callaway, and S. Dhar, *ibid.* **30**, 1724 (1984).

⁴D. M. Cox, D. J. Trevor, R. L. Whetten, E. A. Rohlfing, and A. Kaldor, *Phys. Rev. B* **32**, 7290 (1985).

⁵D. W. Ball, R. G. S. Pang, and Z. H. Kafafi, *J. Am. Chem. Soc.* **115**, 2864 (1993).

⁶H. Poppa, C. A. Papageorgopolous, F. Marks, and E. Bauer, *Z. Phys. D* **3**, 279 (1986).

⁷L. Lozzi, M. Passacantando, P. Pieozzi, S. Santucci, and M. De Crescenzi, *Z. Phys. D* **20**, 387 (1991).

⁸G. K. Wertheim, S. B. Di Cenzo, and D. N. E. Buchanan, *Phys. Rev. B* **33**, 5384 (1986).

⁹T. R. Ohno, Y. Chen, S. E. Harvey, G. H. Kroll, P. J. Benning, J. H. Weaver, L. P. F. Chibante, and R. E. Smalley, *Phys. Rev. B* **47**, 2389 (1993); T. R. Ohno, G. H. Kroll, J. H. Weaver, L. P. F. Chibante and R. E. Smalley, *ibid.* **46**, 10437 (1992).

¹⁰J. Colbert, A. Zangwill, M. Strongin, and S. Krummacher, *Phys. Rev. B* **27**, 158 (1983).

¹¹D. Spanjaard, C. Guillot, M. C. Desjonqueres, G. Treglia, and J. Lecante, *Surf. Sci. Rep.* **5**, 1 (1986).

¹²D. A. Shirley, R. C. Martin, S. P. Kowalczyk, F. R. McFeely, and L. Ley, *Phys. Rev. B* **15**, 544 (1977).

¹³B. Johansson and N. Mårtensson, *Phys. Rev. B* **21** 4427 (1980).

¹⁴B. Sinković, P. D. Johnson, N. B. Brookes, A. Clarke, and N. V. Smith, *Phys. Rev. Lett.* **65**, 1647 (1990).

¹⁵R. J. Lad and V. Henrich, *Phys. Rev. B* **39**, 478 (1989).

¹⁶V. Murgai, S. Raaen, M. Strongin, and R. F. Garrett, *Phys. Rev. B* **33**, 4345 (1986).

¹⁷R. C. Haddon, A. F. Hebard, M. J. Rossensky, D. W. Murphy, S. H. Glarum, T. T. M. Palstra, A. P. Ramirez, S. J. Duclos, R. M. Flemming, T. Siegrist, and R. Tycho, in *Fullerenes: Synthesis, Properties and Chemistry of Large Carbon Clusters*, edited by G. S. Hammond and V. J. Kuck, ACS Symposium Series Vol. 481 (American Chemical Society, Washington, DC, 1992).

¹⁸J. H. Weaver, J. L. Martins, T. Komeda, Y. Chen, T. R. Ohno, G. H. Kroll, N. Troullier, R. E. Haufler, and R. E. Smalley, *Phys. Rev. Lett.* **66**, 1741 (1991).

¹⁹P. J. Benning, D. M. Poirier, T. R. Ohno, Y. Chen, M. B. Jost, F. Stepaniak, G. H. Kroll, J. H. Weaver, J. Fure, and R. E. Smalley, *Phys. Rev. B* **45**, 6899 (1992).

²⁰D. A. Papaconstantopoulos, *Handbook of the Band Structure of Elemental Solids* (Plenum, New York, 1986), p. 291.

²¹G. M. Pastor, J. Dorantes-Davila, and K.-H. Bennemann, *Phys. Rev. B* **40**, 7642 (1989).

²²G. M. Pastor, J. Dorantes-Davila, and K.-H. Bennemann, *Physica B* **149**, 22 (1988).

²³P. A. Montano, J. Zhao, M. Ramanatha, G. K. Shenoy, and W. Schulze, *Z. Phys. D* **12**, 103 (1989).

²⁴J. Colbert, Ph. D thesis, State University of New York at Stony Brook, 1984.